Chapitre 2 : L'ADAMTS2 dans les processus de réparation tissulaire

2.A FIBROSE HEPATIQUE

1. Introduction

Une grande variété d'agents pathogènes, d'origine chimique ou virale, sont susceptibles d'induire des lésions chroniques du foie menant à la formation et au dépôt excessif d'un tissu cicatriciel largement composé de protéines matricielles, en particulier des collagènes fibrillaires. Cette fibrose cicatricielle pourra *in fine* détériorer la fonction hépatique. A l'heure actuelle, il n'existe pas de thérapie efficace pour lutter contre la fibrose. Dans notre étude, nous avons évalué l'effet anti-fibrotique potentiel de l'inhibition de l'ADAMTS2 dans un modèle de fibrose hépatique induite chez les souris déficientes en ADAMTS2 ($TS2^{-/-}$). Notre hypothèse considérait que l'altération de la structure et de la qualité des fibres de collagène déposées pourrait conduire à la formation d'un tissu cicatriciel moins dense au niveau des lésions hépatiques et donc plus enclin aux processus de dégradation du remodelage physiologique.

2. Résumé des résultats

- La réaction aiguë induite par une injection unique de CCl_4, se traduisant par une nécrose centrolobulaire et sa résolution endéans 4 jours, est identique dans les souris de type sauvage (WT) et $TS2^{-/-}$. De même, les variations du niveau d'expression de gènes connus pour leur implication dans la fibrose hépatique, tels que TGF-β1, CTGF, α-actine de type musculaire lisse (α-SMA), les collagènes fibrillaires I, III et V, les enzymes de dégradation de la matrice (MMPs) et leurs inhibiteurs (TIMPs), sont similaires à 1 et 4 jours dans les deux génotypes (Fig. 24).

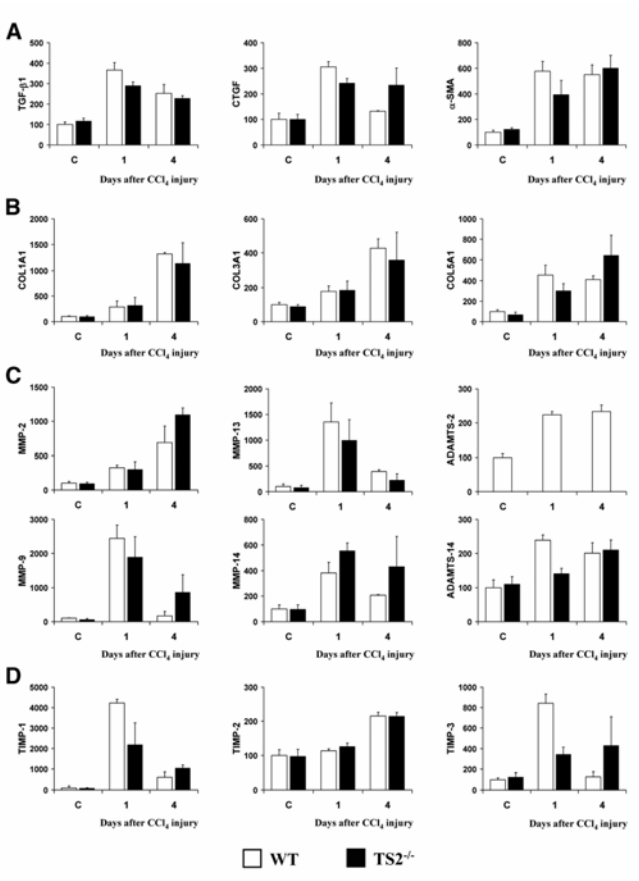

Fig. 24.

Le niveau d'ARNm de gènes participant à la fibrogenèse a été mesuré 1 et 4 jours après une injection unique de CCl_4 dans les souris de type sauvage (WT) et déficientes en ADAMTS2 ($TS2^{-/-}$).

- La fibrose hépatique induite par injections chroniques de CCl_4, et évaluée par coloration au rouge Sirius et dosage du collagène, est réduite chez les souris $TS2^{-/-}$ par rapport aux WT, et ce, pour deux doses d'inducteur et différents temps de traitement (Fig. 25).

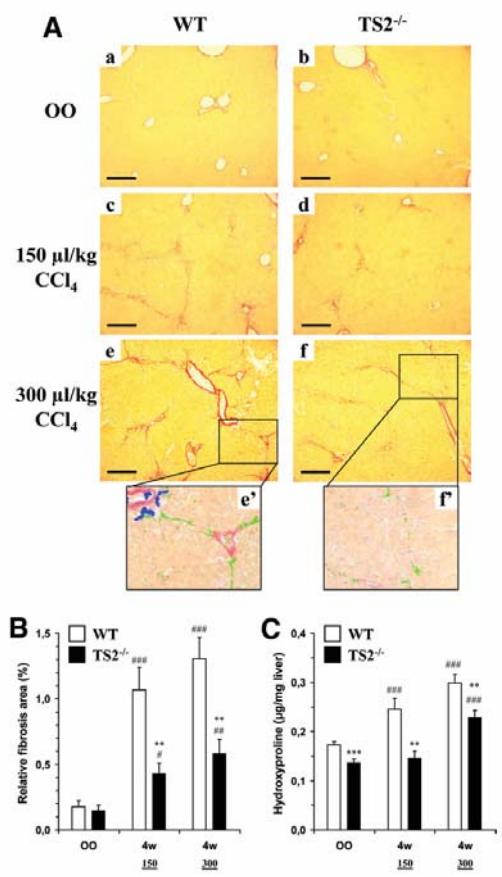

Fig. 25.

A. *Images représentatives de coupes de foie, colorées au rouge Sirius, provenant de souris de type sauvage (WT) ou déficientes en ADAMTS2 ($TS2^{-/-}$) et traitées par injection chronique de CCl_4 à 2 concentrations (150 et 300 µl/kg) ou avec le véhicule seul (OO).* ***B.*** *Une quantification des travées colorées en rouge, par analyse d'image après suppression du marquage des vaisseaux sanguins, objective la réduction visuelle dans les foies des souris $TS2^{-/-}$.* ***C.*** *Le contenu en collagène, déterminé par mesure de l'hydroxyproline, confirme la réduction du dépôt de collagène chez les souris $TS2^{-/-}$.*

- Afin d'évaluer la vitesse de régression des dépôts fibrotiques, des souris WT et TS2$^{-/-}$ ont reçu des injections de CCl_4 pendant respectivement 2 et 4 semaines afin d'atteindre des niveaux de fibrose comparables dans les deux groupes d'animaux. Une semaine après l'arrêt du traitement, la régression des lésions s'est révélée légèrement mais significativement plus rapide chez les souris TS2$^{-/-}$ (-68 %) que chez les souris sauvages (-54 %) (Fig. 26).

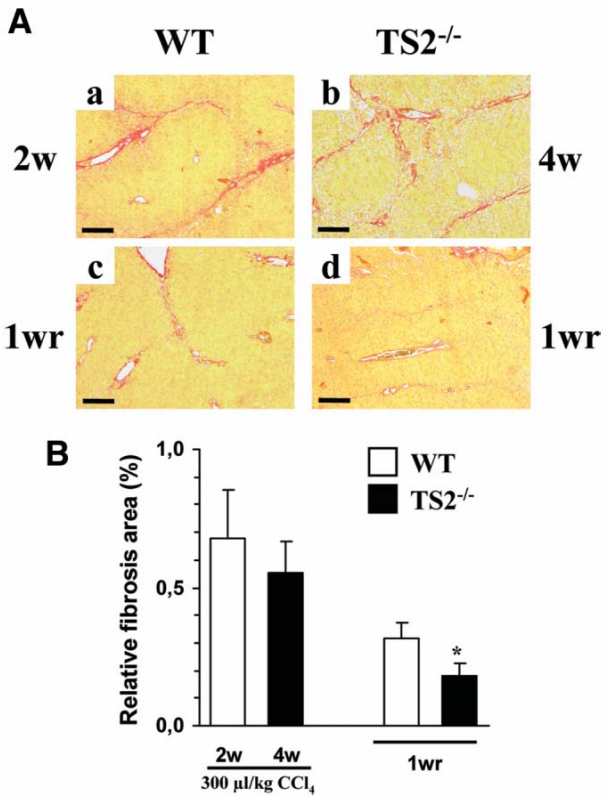

Fig. 26.

A. *Images représentatives de colorations au rouge Sirius de coupes de foie de souris sauvages (WT) et déficientes en ADAMTS2 (TS2$^{-/-}$) traitées respectivement durant 2 (2w) et 4 semaines (4w) par des injections chroniques de CCl_4, période suivie d'une semaine de récupération (1WR).* ***B.*** *Quantification par analyse d'image des septa fibreux après exclusion des vaisseaux sanguins.*

- Après administration chronique de CCl_4 durant 4 semaines chez les souris WT, une expression fortement accrue de la plupart des gènes impliqués dans la réaction fibrotique (collagènes I, III et V, les MMP2, 9, 13 et 14, l'ADAMTS2 et 14 ainsi que les TIMPs) est observée à l'exception de TGF-β1, CTGF et l'α-SMA qui ne sont accrus que dans la réaction aiguë. Des modifications similaires sont observées chez les souris TS2$^{-/-}$. Lors de la cessation du traitement fibrogénique, un retour progressif vers un niveau normal d'expression de ces différents gènes est noté de manière identique pour les deux types de souris.

- L'analyse ultrastructurale du collagène déposé dans le foie montre un réseau de fibres moins abondant et moins compact dans les souris TS2$^{-/-}$. Les fibres présentent un contour légèrement irrégulier et un diamètre significativement réduit en coupe transversale. Le

profil électrophorétique des polypeptides de collagène déposés dans le foie montre une proportion significative de pNcollagène de type I et de type III dans les foies fibrotiques des souris $TS2^{-/-}$, alors que la maturation est pratiquement complète chez les souris WT.

3. Conclusions

Alors que tous les paramètres de réactivité aiguë et chronique envers l'agent hépatotoxique sont similaires chez les souris $TS2^{-/-}$ et de type sauvage, nous avons clairement démontré que la fibrose développée en absence de l'ADAMTS2 est moins étendue en raison d'une réduction de la vitesse de dépôt de fibres de collagène qui, par ailleurs, sont mal structurées. En effet, la persistance des aminopropeptides lors de la polymérisation des molécules de collagène introduit une interférence stérique responsable de la formation de fibres plus fines et moins compactes, et donc plus enclines à la dégradation par les collagénases. L'inhibition de la maturation des collagènes fibrillaires pourrait être une approche thérapeutique bénéfique permettant d'interférer avec le développement et la persistance des lésions fibrotiques.

ADAM Metallopeptidase with Thrombospondin Type 1 Motif 2 Inactivation Reduces the Extent and Stability of Carbon Tetrachloride–Induced Hepatic Fibrosis in Mice

Frédéric Kesteloot,[1] Alexis Desmoulière,[2,3] Isabelle Leclercq,[4] Marc Thiry,[5] Jorge E. Arrese,[6] Darwin J. Prockop,[7] Charles M. Lapière,[1] Betty V. Nusgens,[1] and Alain Colige[1]

ADAMTS2 belongs to the "ADAM metallopeptidase with thrombospondin type 1 motif" (ADAMTS) family. Its primary function is to process collagen type I, II, III, and V precursors into mature molecules by excising the aminopropeptide. This process allows the correct assembly of collagen molecules into fibrils and fibers, which confers to connective tissues their architectural structure and mechanical resistance. To evaluate the impact of ADAMTS2 on the pathological accumulation of extracellular matrix proteins, mainly type I and III collagens, we evaluated carbon tetrachloride–induced liver fibrosis in ADAMTS2-deficient ($TS2^{-/-}$) and wild-type (WT) mice. A single carbon tetrachloride injection caused a similar acute liver injury in deficient and WT mice. A chronic treatment induced collagen deposition in fibrous septa that were made of thinner and irregular fibers in $TS2^{-/-}$ mice. The rate of collagen deposition was slower in $TS2^{-/-}$ mice, and at an equivalent degree of fibrosis, the resorption of fibrous septa was slightly faster. Most of the genes involved in the development and reversion of the fibrosis were similarly regulated in $TS2^{-/-}$ and WT mice. *Conclusion:* These data indicate that the extent of fibrosis is reduced in $TS2^{-/-}$ mice in comparison with their WT littermates. Inhibiting the maturation of fibrillar collagens may be a beneficial therapeutic approach to interfering with the development of fibrotic lesions. (HEPATOLOGY 2007;46:1620-1631.)

Abbreviations: 1wr, 1 week of recovery; 2w, 2 weeks; 4w, 4 weeks; α-SMA, alpha-smooth muscle actin; α1(III), α1 chain of type III collagen; ADAMTS, ADAM metallopeptidase with thrombospondin type 1 motif (as defined in the National Center for Biotechnology Information databank for both gene and protein); ALT, alanine aminotransferase; AST, aspartate aminotransferase; BDL, bile duct ligation; C, control; CCl_4, carbon tetrachloride; CPS, carbamyl phosphate synthase; CTGF, connective tissue growth factor; CV, centrilobular vein; ECM, extracellular matrix; MMP, matrix metalloproteinase; mRNA, messenger RNA; NI, not injected; N-propeptide, aminopropeptide; OO, olive oil; pNα, α chain containing the aminopropeptide; pNcollagen, aminoprocollagen; PSR, picrosirius red; PT, portal tract; RT-PCR, reverse-transcription polymerase chain reaction; SEM, standard error of the mean; TGF-β1; transforming growth factor-beta 1; TIMP, tissue inhibitor of metalloproteinases; $TS2^{-/-}$, ADAMTS2-deficient; WT, wild type.

From the [1]Laboratory of Connective Tissues Biology, Interdisciplinary Cluster for Applied Genoproteomics/Center for Experimental Cancer Research, University of Liège, Liège, Belgium; [2]Groupe de Recherches pour l'Etude du Foie, Institut National de la Santé et de la Recherche Médicale E0362, Université Victor Segalen Bordeaux 2, Bordeaux, France; [3]Department of Physiology, Faculty of Pharmacy, University of Limoges, Limoges, France; [4]Gastroenterology Unit, Université Catholique de Louvain, Brussels, Belgium; [5]Laboratoire de Biologie Cellulaire et Tissulaire, Université de Liège, Liège, Belgium; [6]Department of Dermatopathology, University Hospital of Liège, Sart Tilman, Belgium; and [7]Center for Gene Therapy, Tulane University Health Science Center, New Orleans, LA.

Received December 22, 2006; accepted June 11, 2007.

Supported by the Belgian Fonds National de la Recherche Scientifique (Télévie grants 7.4541.01, 7.4561.03, and 7.4566.05), the Belgian Fonds de la Recherche Scientifique Médicale (grants 3.4362.03 and 3.4387.05), the Belgian Federation Against Cancer (nonprofit organization), the European Commission through the Sixth Framework Programme for CORNEA ENGINEERING (contract NMP2-CT-2003-504017), and the Région Wallonne through the Réseaux Programme for FIBROMED (contract 415907).

Address reprint requests to: Alain Colige, Laboratory of Connective Tissues Biology, Tour de Pathologie, B23/3, 4000 Sart Tilman, Belgium. E-mail: acolige@ulg.ac.be; fax: 32-4-366-2457.

Published online in Wiley InterScience (www.interscience.wiley.com).

DOI 10.1002/hep.21868

Potential conflict of interest: Dr. Prockop owns stock in FibroGen.

Supplementary material for this article can be found on the HEPATOLOGY Web site (http://interscience.wiley.com/jpages/0270-9139/suppmat/index.html).

Chronic damage to the liver in a variety of conditions leads to scar formation resulting from an increased deposition of extracellular matrix (ECM) proteins. The main component of the newly formed ECM is collagen.[1] Ultimately, hepatic fibrosis leads to cirrhosis, which is characterized by a pathological accumulation of fibrous tissue impairing hepatic function by the disruption of the organ structure[2] and abnormal interactions with resident liver cells. The loss of differentiated functions of hepatocytes and the reduction of sinusoidal cell porosity, leading to the reduced transport of solutes from sinusoidal blood to the subendothelial space, can collectively explain the metabolic dysfunction characteristic of advanced liver disease.[3] Currently, no specific therapy for fibrosis is available. Two approaches aimed at the reduction of excessive scar formation are theoretically possible. The first would consist of the stimulation of specific proteolytic pathways in order to accelerate the degradation of the excessive ectopic ECM. The second would be aimed at inhibiting the synthesis of the fibrous extracellular macromolecules and/or altering their structure. This would result in the deposition of defective scar tissue prone to rapid degradation by physiological remodeling processes. Despite the complex regulatory events leading to fibrosis, the biosynthesis of collagen is a well-defined process, and this makes it a suitable target for therapeutic intervention.[4] Its turnover in normal adult tissues is quite slow in comparison with the active remodeling occurring in liver fibrosis, which should minimize side effects of the therapy.

The most abundant fibrillar collagens accumulating during the fibrotic process are type I and type III collagens.[5,6] They are synthesized as precursors (procollagens) formed by a central triple-helix domain extended by propeptides at both extremities. The final step in the post-translational processing of procollagen molecules is the cleavage of the C-propeptide by bone morphogenetic protein-1 and related mammalian tolloid-like 1 metalloproteinases with an astacin-like protease domain.[7,8] This cleavage is followed by the excision of the aminopropeptide (N-propeptide) by aminoprocollagen (pNcollagen) peptidases[9] now identified as ADAMTS2,[10] ADAMTS3,[11] and ADAMTS14,[12] 3 closely related metalloproteinases that belong to the "ADAM metallopeptidase with thrombospondin type 1 motif" (ADAMTS) family. Removal of the propeptides is required to generate collagen monomers able to assemble into elongated and cylindrical collagen fibrils to form compact bundles, which confer to the connective tissues mechanical resistance and informational properties. For example, the copolymerization of pNcollagen type I (collagen I that retains its aminoterminal extension) with fully processed type I collagen results in altered fibril organization both *in vitro*[13,14] and *in vivo*.[15] ADAMTS2 is responsible for most of the pN-collagen type I processing[9,16-18] and is able to process pN-collagen type II in cartilage.[11,19] Recently, it has been shown that ADAMTS2 is also able to process pNcollagen types III[20] and V.[21] As ADAMTS2 is a key regulator of procollagen maturation and collagen fibril formation, its inhibition should affect collagen deposition and scar tissue stability.

In this study, the potential antifibrotic effect of the inhibition of ADAMTS2 was investigated with an *in vivo* model of liver fibrosis induced by the administration of carbon tetrachloride (CCl_4) in ADAMTS2-deficient ($TS2^{-/-}$) mice in comparison with wild-type (WT) littermates.

Materials and Methods

Animals and Administration of CCl_4. The generation and characterization of $TS2^{-/-}$ mice of the 129SVJ strain have been described.[22] Mice were maintained under standard laboratory conditions, with 12-hour light/12-hour dark cycles and free access to food and water at all stages of the experiments. For acute CCl_4-induced liver injury, a single CCl_4 dose of 150 μL/kg of body weight (Fluka Chemika, Buchs, Switzerland) as a 3% (vol/vol) solution in olive oil (OO) was administered by intraperitoneal injection, the control animals being not injected (NI). For chronic CCl_4-induced liver fibrosis, a CCl_4 dose of 150 μL/kg of body weight as a 3% (vol/vol) solution in OO or a CCl_4 dose of 300 μL/kg of body weight as a 6% (vol/vol) solution in OO was injected intraperitoneally 3 times a week for 4 weeks. Control animals were injected with OO alone. In some experiments, mice were induced with 300 μL/kg CCl_4 for 4 weeks and sacrificed 4 (peak fibrosis), 11 (1 week of recovery), or 18 days (2 weeks of recovery) after the last injection. In other reversal experiments, in order to induce a similar degree of fibrosis in both types of mice, WT mice were injected for 2 weeks and $TS2^{-/-}$ mice were injected for 4 weeks with CCl_4 (300 μL/kg) and then sacrificed 4 (peak fibrosis) or 11 days (1 week of recovery) after the last injection. Groups of age-matched and sex-matched WT or $TS2^{-/-}$ mice were sacrificed at the indicated times. After anesthesia and exsanguination, livers were collected and weighed. One lobe was fixed in 4% formalin for histological analyses, and the other was sampled according to a standardized procedure and frozen for biochemical and molecular biological analyses. All procedures were performed in accordance with the institutional, Federation of European Laboratory Animal Science Associations, and American National Institutes of Health guidelines for animal care.

Bile Duct Ligation (BDL) Model. WT and TS2$^{-/-}$ mice were subjected to BDL as described.[23] Briefly, the common bile duct was double-ligated after a midline abdominal incision. The animals were sacrificed 9 days after BDL, and their livers were collected for morphological studies.

Measurement of the Collagen Content. A frozen piece of the left lobe of the liver was lyophilized, weighed, and hydrolyzed in 6 M hydrochloric acid at 137°C for 3 hours. The collagen content was estimated from hydroxyproline measured with the technique of Bergman and Loxley.[24] The hydroxyproline assays performed on 1 lobe were validated by a comparison with measurements performed on a pool of 3 lobes in a series of untreated and CCl_4-treated WT and TS2$^{-/-}$ mice (not shown).

Immunohistochemistry. Sections (5 μm) were stained with hematoxylin/eosin for a general histology and necrosis assessment and immunostained with a mouse monoclonal antibody against alpha-smooth muscle actin (α-SMA; 1/100; Dako, Glostrup, Denmark) biotinylated with an animal research kit (Dako). The quantification of α-SMA–positive cells was performed in 10 fields per liver, focused on the border of a centrilobular vein, in CCl_4-treated WT (n = 4) and TS2$^{-/-}$ mice (n = 5).

Quantitative Image Analysis of Picrosirius Red (PSR) Staining. Fibrosis was evaluated in WT and TS2$^{-/-}$ mice by the quantitative image analysis of sections stained with PSR to visualize collagen fibers.[25] Images were acquired with a Zeiss Axiovert 25 microscope (Carl Zeiss Microscopy, Jena, Germany) equipped with an AxioCam camera, and quantitative data were obtained with the KS 400 imaging system. The analysis was performed on 6 fields per section with a 10× objective. Stained vessel walls were systematically excluded to quantify only the fibrotic scar septa [overlaid by green pixels; see Fig. 4A, panels e′ and f′ (shown later)]. Fibrosis was expressed as the mean percentage of the PSR-stained areas of the total field tissue area.

Western Blotting Analysis. Liver samples were homogenized on ice in an aqueous solution containing a cocktail of protease inhibitors [3 tablets (Complete Mini, Roche) in 20 mL of 5 mM ethylenediamine tetraacetic acid, 2.5 mM N-ethylmaleimide, and 0.5 mM phenylmethylsulfonyl fluoride]. An aliquot of the total homogenate was mixed with the same volume of a 2× concentrated Laemmli buffer and heated at 65°C for 15 minutes. An amount of lysate equivalent to 0.5 (for collagen I) or 2.25 mg of liver (for collagen III) was electrophoresed under nonreducing (for collagen I) or reducing conditions (50 mM dithiothreitol for collagen III) on a 7.5% sodium dodecyl sulfate–polyacrylamide gel according to the technique of Laemmli.[26] Western blotting was performed as described.[27] Some gels were stained with Coomassie blue to visualize carbamyl phosphate synthase (CPS), which was used as a standard to monitor the protein loading. The polyvinylidene difluoride membranes were probed with a rabbit antiserum directed against type I collagen (1/3000) or with a guinea pig antiserum directed against type III collagen (1/4000).[28] The secondary peroxidase-conjugated antibodies were swine anti-rabbit immunoglobulin (1/2000; P0217, Dako) and rabbit anti–guinea pig immunoglobulin (1/2000; P0141, Dako). Peroxidase was revealed with an enhanced chemiluminescence assay (Amersham Biosciences, Ltd., England) and X-ray film exposure.

RNA Purification and Reverse-Transcription Polymerase Chain Reaction (RT-PCR) Analysis. The total RNA was extracted from the whole liver with a NucleoSpin RNA II kit (Macherey-Nagel, Düren, Germany), according to the manufacturer's recommendations. The RT-PCR amplifications were performed in an automated thermocycler (GeneAmp PCR System 9700, Applied Biosystems, Foster City, CA) with a GeneAmp Thermostable r*Tth* Reverse Transcriptase RNA PCR Kit (Applied Biosystems, Foster City, CA). Primer sequences of genes used for the quantification of messenger RNA (mRNA) levels by RT-PCR are listed in Supplementary Table 1. For the α1 chain of type III collagen [α1(III)], matrix metalloproteinase-2 (MMP-2), MMP-9, MMP-13, MMP-14, tissue inhibitor of metalloproteinases-3 (TIMP-3), and 28S ribosomal RNA, the efficiency of RT-PCR was controlled by a synthetic RNA cotranscribed and coamplified with the same primers as the endogenous RNA to yield an amplification product of a larger size.[29,30] The RT-PCR products were quantified after electrophoresis on a 10% polyacrylamide gel and staining (Gelstar, FMC BioProducts) with a Fluor-S MultiImager (Life Science, Bio-Rad Laboratories) and normalized as a ratio to 28S ribosomal RNA. For all investigated genes, the mRNA levels were similar in control groups subjected to acute (NI mice) and chronic (4 weeks of OO) treatments, and this allowed us to pool the NI and OO groups for statistical tests.

Blood Enzyme Analyses. As a quantitative measure of liver injury by CCl_4, the activity of alanine aminotransferase (ALT) and aspartate aminotransferase (AST) in the serum was determined with commercially available kits (ALT [ALAT/GPT] for ALT and AST (ASAT/GOT) for AST, Roche, Mannheim, Germany) according to the manufacturer's instructions.

Electron Microscopy. Fragments of livers from WT and TS2$^{-/-}$ mice were fixed for 60 minutes at room temperature in 2.5% glutaraldehyde in Sörensen's buffer (0.1 M, pH 7.4), postfixed for 30 minutes in 0.1% osmium tetroxide in the same buffer, dehydrated

in a series of ethanol concentrations, and embedded in an epoxy resin (Epon 812, Fluka). Ultrathin sections were stained with uranyl acetate and lead citrate before being examined with a JEOL CX100 II electron microscope at 60 kV. The measurement of the diameter of at least 10 fibers in a transverse section per photograph was performed for at least 4 micrographs per group of mice (n = 2).

Zymography. Liver samples were ground into liquid nitrogen, homogenized in an extraction buffer [50 mM trishydroxymethylaminomethane, 0.1% Brij, 2 M urea, 1 M NaCl (pH 7.6), and 0.1 mM phenylmethylsulfonyl fluoride] and centrifuged. The supernatant was dialyzed 3 times against 50 mM trishydroxymethylaminomethane, 0.1% Brij, 10 mM $CaCl_2$ (pH 7.6), and 0.1 mM phenylmethylsulfonyl fluoride, and the total protein content was assessed with a bicinchoninic acid assay (Micro BCA Protein Assay Kit, Pierce, Rockford, IL). Equal amounts of proteins were loaded onto gelatin sodium dodecyl sulfate–polyacrylamide gels, and zymography was performed as described.[30]

Statistical Analysis. Animals were randomly assigned to control and treatment groups. The results are presented as the means ± the standard error of the mean (SEM). The significance of the differences between means was assessed with a 2-tailed Student *t* test or a Mann-Whitney test, when appropriate. $P < 0.05$ was considered significant.

Results

ADAMTS2 Deficiency Does Not Alter the Acute Reactivity to Liver Injury Induced by a Single CCl_4 Injection. In order to determine whether the absence of ADAMTS2 had any influence on the acute liver response to CCl_4 exposure, the extent of the initial necrotic reaction and its resolution were analyzed after a single dose of CCl_4 (Fig. 1). In both WT and $TS2^{-/-}$ mice, centrilobular necrotic lesions were already present on day 1, peaked on day 2, and had almost completely recovered on day 4 after the CCl_4 treatment. After 7 days, inflammatory cells were almost absent. At all investigated times, no histological difference could be found between WT and $TS2^{-/-}$ mice. Consistent with these results, both the ALT and AST activities, hallmarks of liver injury,[31] measured in the serum (Fig. 2) showed similar peaks in WT and $TS2^{-/-}$ mice 1 day after CCl_4 administration that rapidly and similarly vanished.

The expression of several genes related to connective tissue synthesis, maturation, and remodeling was assessed with RT-PCR. The level of mRNA coding for transforming growth factor-beta 1 (TGF-β1), connective tissue growth factor (CTGF), and α-SMA (Fig. 3A) was already up-regulated on day 1 to similar extents in WT and $TS2^{-/-}$ mice and remained elevated on day 4. The

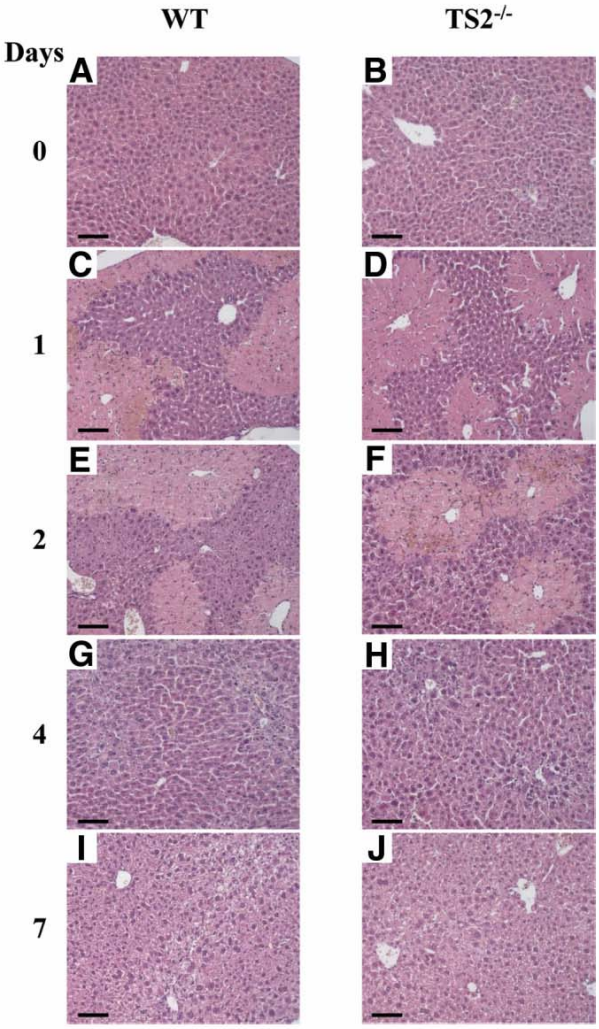

Fig. 1. The extent of CCl_4-induced hepatic necrosis and its resolution are similar in WT and $TS2^{-/-}$ mice. (A-J) Representative photographs of hematoxylin/eosin staining of liver tissue sections are shown (scale bars: 100 μm). (A,C,E,G,I) WT and (B,D,F,H,J) $TS2^{-/-}$ mice were (A,B) not injected or injected once with 150 μL/kg CCl_4 and sacrificed after (C,D) 1 day, (E,F) 2 days, (G,H) 4 days, or (I,J) 7 days.

mRNA of fibrillar collagen types I, III, and V (Fig. 3B) started to increase on day 1, the maximal increase being observed after 4 days. Enzymes involved in the processing and maturation of procollagen (ADAMTS2 in WT mice and ADAMTS14 in WT and $TS2^{-/-}$ mice), the proteolytic enzymes (MMP-2, MMP-9, MMP-13, and MMP-14; Fig. 3C) and some of their inhibitors (TIMP-1, TIMP-2, and TIMP-3; Fig. 3D) were also up-regulated on days 1 and 4 following liver injury. ADAMTS3 expression was not detected in the liver. The strongest induction for both genotypes was observed for MMP-9 and TIMP-1 (see the scale). Except for ADAMTS14 and TIMP-3 after 1 day, no significant difference was observed between WT and $TS2^{-/-}$

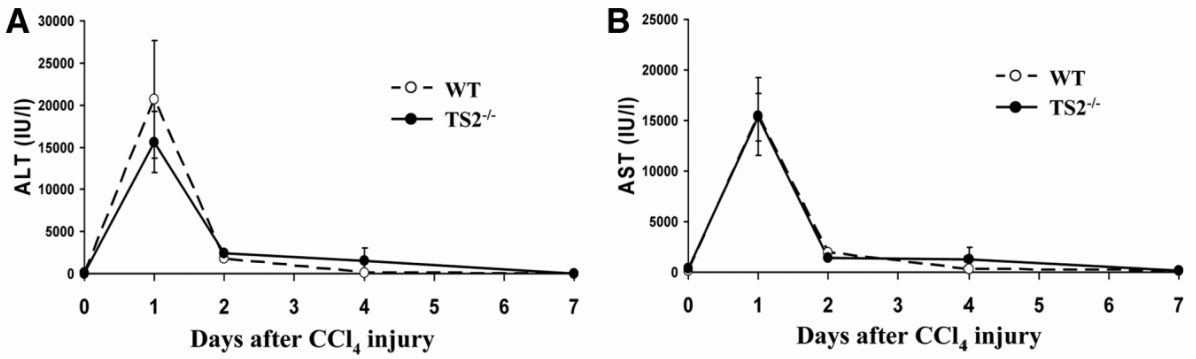

Fig. 2. The lack of ADAMTS2 activity does not modulate the serum ALT and AST levels following the injection of CCl_4. (A) ALT and (B) AST activity in serum collected from (○) WT and (●) $TS2^{-/-}$ mice at the indicated times after a single injection of CCl_4 (150 μL/kg). The ALT and AST levels are shown as international units per liter ± the SEM. Each time represents the mean value measured in a minimum of 3 animals, except at days 4 and 7 (n = 2). No difference was observed between WT and $TS2^{-/-}$ mice at any time.

mice at any time and for any of the investigated genes, and this means that an ADAMTS2 deficiency does not modify the acute reactivity to liver injury.

Hepatic Fibrosis Is Reduced in TS2$^{-/-}$ Mice. After chronic injections of CCl_4 for 4 weeks, the ALT and AST levels were slightly but similarly up-regulated in WT and $TS2^{-/-}$ mice (data not shown). A histological evaluation of hepatic tissues after PSR staining indicated that WT and $TS2^{-/-}$ mice that were NI (not shown) or were injected with OO alone (Fig. 4A, panels a and b) displayed similar basal amounts of fibrous collagen staining restricted to the vessel walls. After chronic injections with CCl_4 (Fig. 4A, panels c and e), WT developed fibrous septa around the centrilobular veins that were already quite visible at the lowest concentration of CCl_4 (150 μL/kg) and accentuated at the highest dosage (300 μL/kg). In contrast, the collagen deposition in $TS2^{-/-}$ mice injected with the same amount of CCl_4 (Fig. 4A, panels d and f) was less dense. Digital image analysis (Fig. 4A, panels e′ and f′) was used to quantify the stained hepatic collagen accumulating specifically in newly formed scar septa after the systematic exclusion of the stained vessel walls. This quantification (Fig. 4B) confirmed the visual observation that a lower collagen accumulation occurred in $TS2^{-/-}$ animals versus WT animals. The extent of collagen deposition was also compared between males and females during the development of the fibrosis. No significant difference was observed at any investigated time for

Table 1. Steady-State Levels of mRNAs After CCl_4 Administration in WT and $TS2^{-/-}$ Livers and During the Reversal of Fibrosis

		Control (OO + NI)		4 Weeks of CCl_4 (300 μL/kg)		+1 Week of Recovery		+2 Weeks of Recovery	
		WT	$TS2^{-/-}$	WT	$TS2^{-/-}$	WT	$TS2^{-/-}$	WT	$TS2^{-/-}$
Fibrosis initiation	TGF-β1	100 ± 13	117 ± 13	71 ± 9	98 ± 17	114 ± 13	82 ± 17	125 ± 9	82 ± 22
	CTGF	100 ± 24	100 ± 20	173 ± 20	178 ± 16	230 ± 24	149 ± 44	133 ± 52	99 ± 20
	α-SMA	100 ± 14	121 ± 14	83 ± 21	131 ± 29	173 ± 93	212 ± 121	110 ± 21	187 ± 64
Structural proteins	Colα1(I)	100 ± 12	94 ± 24	1328 ± 203	940 ± 129	605 ± 88	542 ± 12	367 ± 106	486 ± 188
	Colα1(III)	100 ± 13	87 ± 13	471 ± 48	369 ± 19	306 ± 39	267 ± 6	236 ± 39	271 ± 52
	Colα1(V)	100 ± 15	68 ± 25	824 ± 304	374 ± 152	315 ± 127	269 ± 25	162 ± 25	151 ± 15
Proteinases	MMP-2	100 ± 27	92 ± 23	2919 ± 249	2366 ± 226	622 ± 122	477 ± 9	231 ± 50	417 ± 100
	MMP-9	100 ± 12	63 ± 31	248 ± 120	115 ± 12	267 ± 23	202 ± 113	146 ± 18	225 ± 116
	MMP-13	100 ± 53	80 ± 45	1727 ± 1021	736 ± 212	213 ± 45	54 ± 23	201 ± 45	176 ± 68
	MMP-14	100 ± 32	96 ± 36	232 ± 71	144 ± 43	122 ± 28	132 ± 36	118 ± 32	143 ± 71
	ADAMTS2	100 ± 9	–	444 ± 28	–	298 ± 79	–	151 ± 7	–
	ADAMTS14	100 ± 22	109 ± 22	238 ± 44	159 ± 30	126 ± 7	192 ± 30	124 ± 30	101 ± 44
Inhibitors	TIMP-1	100 ± 100	80 ± 32	200 ± 32	416 ± 160	16 ± 16	217 ± 73	112 ± 57	71 ± 46
	TIMP-2	100 ± 17	97 ± 20	278 ± 48	237 ± 54	178 ± 64	201 ± 15	127 ± 20	123 ± 32
	TIMP-3	100 ± 19	127 ± 38	152 ± 5	131 ± 23	129 ± 24	127 ± 20	74 ± 6	95 ± 20

The results (means ± SEM) are expressed as arbitrary units per unit of 28S ribosomal RNA in a percentage of the control WT mice. n was 3-17 in each group, except at 4 weeks + 1 week of recovery, for which n was 2-4. No statistical difference between WT and $TS2^{-/-}$ mice was observed. Obvious differences during the evolution of the process have not been labeled to prevent overloading of the table.

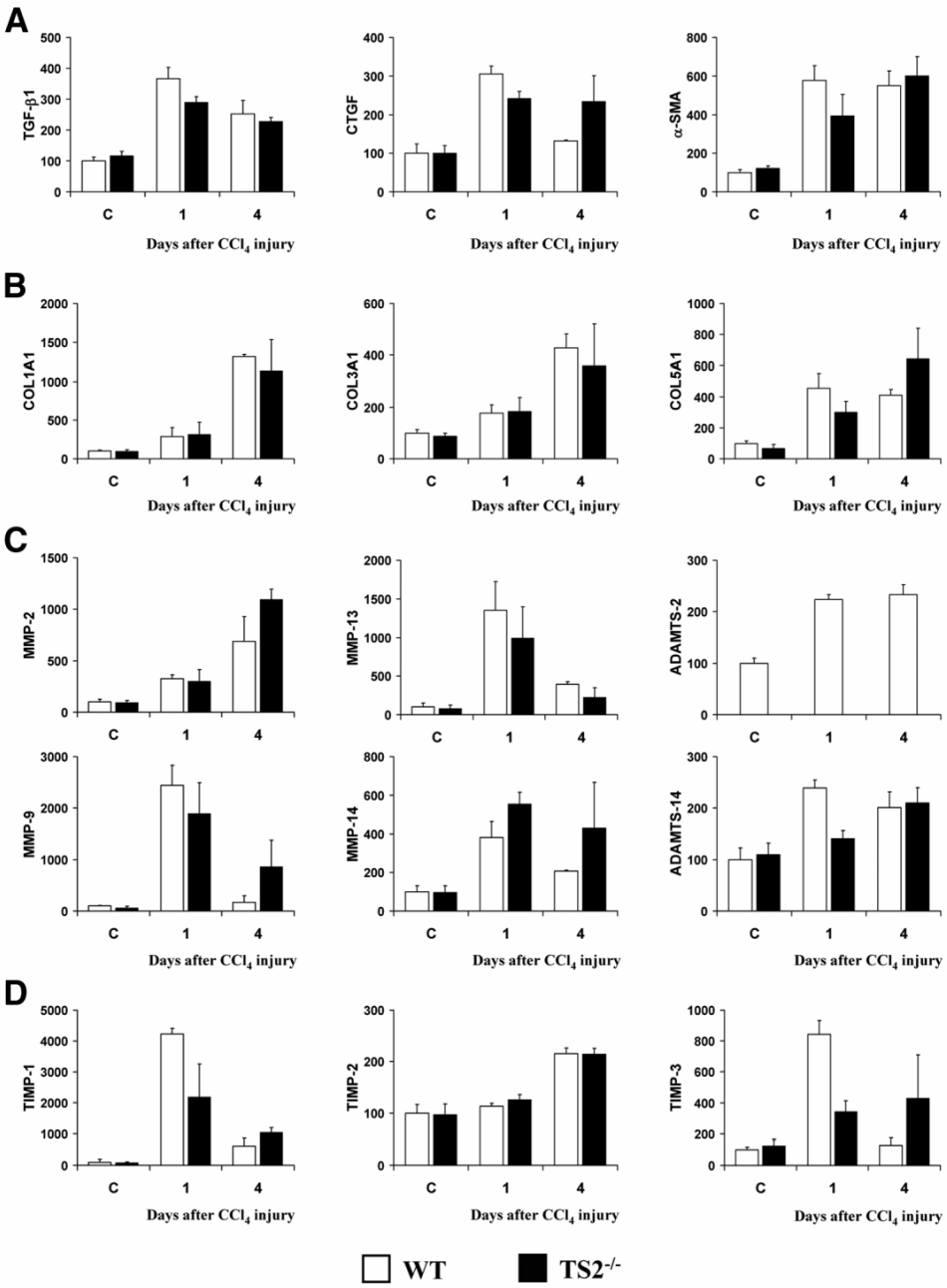

Fig. 3. The genes related to acute toxicity liver injury are similarly modulated in WT and TS2$^{-/-}$ livers. The mRNA expression of several genes related to fibrogenesis was measured in WT (empty bars) and TS2$^{-/-}$ mice (filled bars) 1 and 4 days after a single injection of CCl_4 (150 μL/kg) and in control (C) animals not receiving CCl_4. The investigated genes were related to (A) fibrosis initiation (TGF-β1, CTGF, and α-SMA), (B) fibrillar collagens (types I, III, and V), (C) metalloproteinases (MMP-2, MMP-9, MMP-13, MMP-14, ADAMTS2, and ADAMTS14), and (D) TIMPs (TIMP-1, TIMP-2, and TIMP-3). The results are expressed as the means ($\pm$ the SEM) of groups from 4-11 mice, except at day 4 (n = 2), in a percentage of the control WT mice. No significant difference was observed between the WT and TS2$^{-/-}$ mice for any gene at any time, except for ADAMTS14 and TIMP-3 at day 1.

either WT or TS2$^{-/-}$ mice (data not shown); this allowed us to consider mixed males and females as a group and to compare larger groups of mice from a lower number of litters, improving the statistical strength of the data. The weight of the liver similarly increased by 30% in TS2$^{-/-}$ and WT mice upon a chronic fibrogenic treatment. Despite the elevated background due to the presence of type IV collagen and fibrillar collagens in the vessel walls, hy-

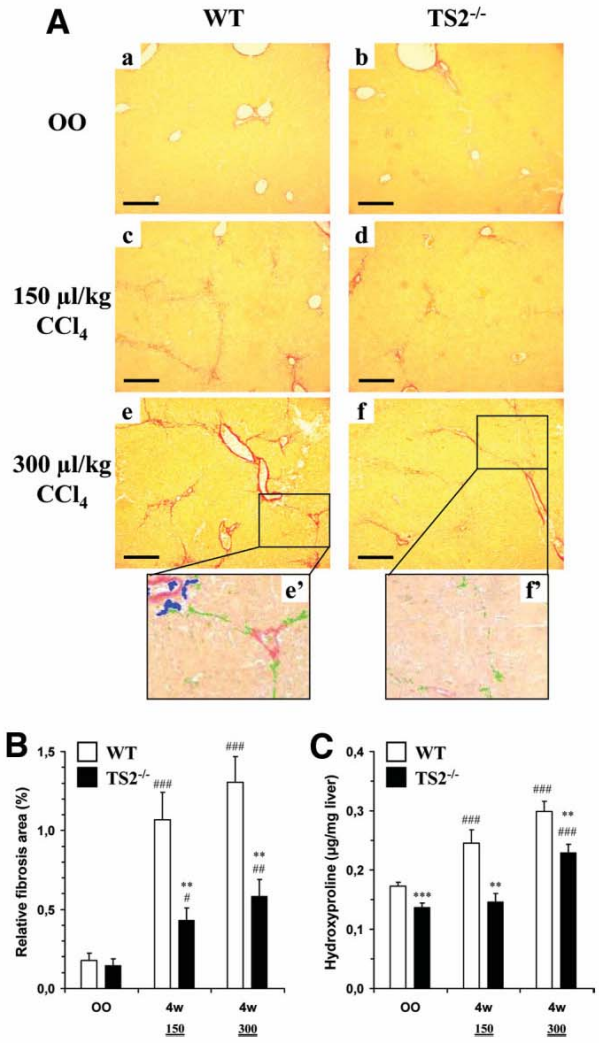

Fig. 4. Reduced fibrosis is observed in TS2$^{-/-}$ mice after chronic CCl_4 administration. (A) Representative PSR staining of liver sections (scale bars: 250 μm). (a) OO-treated WT mouse. (b) OO-treated TS2$^{-/-}$ mouse. (c,e) WT or (d,f) TS2$^{-/-}$ mice were subjected to a chronic CCl_4 treatment at a dose of (c,d) 150 or (e,f) 300 μL/kg in OO as described in the Materials and Methods section. (c-f) Livers were collected after 4 weeks of the chronic treatment. (e',f') Digital image analyses of PSR staining: fibrotic zones (in green, excluding vessel walls) have been normalized to the field tissue surface (in blue, excluding nontissue area). (B) Digital image analysis quantification of PSR staining. The fibrosis areas were measured as described in the Materials and Methods section in WT (empty bars) and TS2$^{-/-}$ mice (filled bars) after 4 weeks of the OO vehicle only or 4 weeks of CCl_4 injected at a dose of 150 or 300 μL/kg, as indicated. The degree of fibrosis was expressed as a mean percentage ($\pm$ the SEM) of the field tissue area. (C) The hydroxyproline content in the livers of WT (empty bars) and TS2$^{-/-}$ mice (filled bars) was assessed in the same samples on a microgram/milligram dry weight basis after 150 or 300 μL/kg CCl_4 exposure as described in the Materials and Methods section. The bars show the means $\pm$ the SEM of groups from 6-36 mice. $^{**}P < 0.01$ and $^{***}P < 0.001$ versus the WT group. $\#P < 0.05$, $\#\#P < 0.01$, and $\#\#\#P < 0.001$ versus the corresponding control group treated with OO.

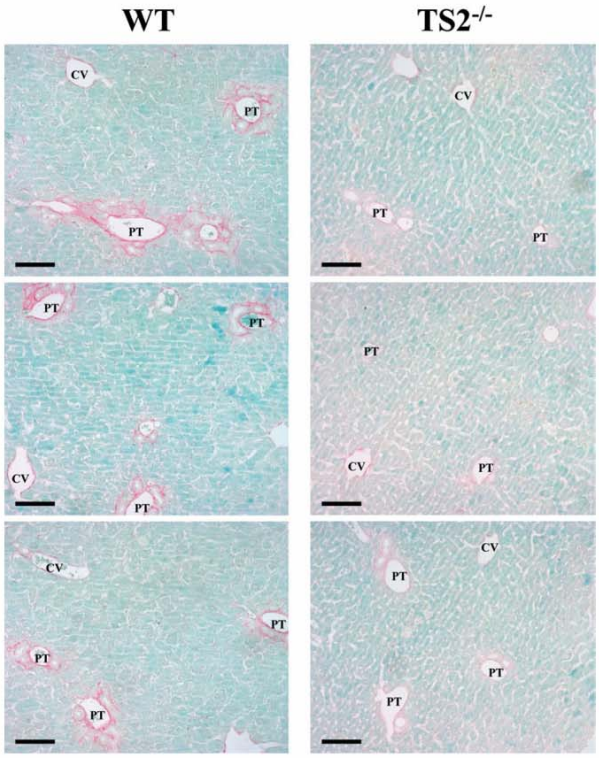

Fig. 5. Portal fibrosis induced by BDL is reduced in TS2$^{-/-}$ mice. PSR staining of liver sections from WT (left side) and TS2$^{-/-}$ mice (right side) 9 days after BDL is shown (scale bars: 100 μm). CV indicates centrilobular vein; and PT, portal tract.

droxyproline measurements (Fig. 4C) confirmed these results, with significantly reduced levels in TS2$^{-/-}$ animals in comparison with WT animals after chronic injections of CCl_4 for 4 weeks.

These results were confirmed with the BDL model. The PSR staining of liver sections from WT and TS2$^{-/-}$ mice 9 days after BDL displayed extensive peribiliary and interstitial collagen staining around portal tracts that was much less intense in TS2$^{-/-}$ mice (Fig. 5).

Fibrosis Reversal Is More Efficient in TS2$^{-/-}$ Mice. Further investigations examined the effects of an ADAMTS2 deficiency on the stability of the fibrosis (Fig. 6) by analyzing livers from cohorts of mice of each genotype after 1 week of recovery following the end of CCl_4 administration. To test more precisely the rate of regression of fibrosis, 2 groups of WT and TS2$^{-/-}$ mice were treated with CCl_4 for 2 and 4 weeks, respectively, to obtain levels of fibrosis as similar as possible. The degree of fibrosis in the TS2$^{-/-}$ mice after 4 weeks of CCl_4 was 80% of that of the WT mice treated for only 2 weeks, supporting a lower rate of collagen deposition in the deficient mice. The regression in the TS2$^{-/-}$ mice was somewhat faster (-68%) than that in the WT mice (-54%).

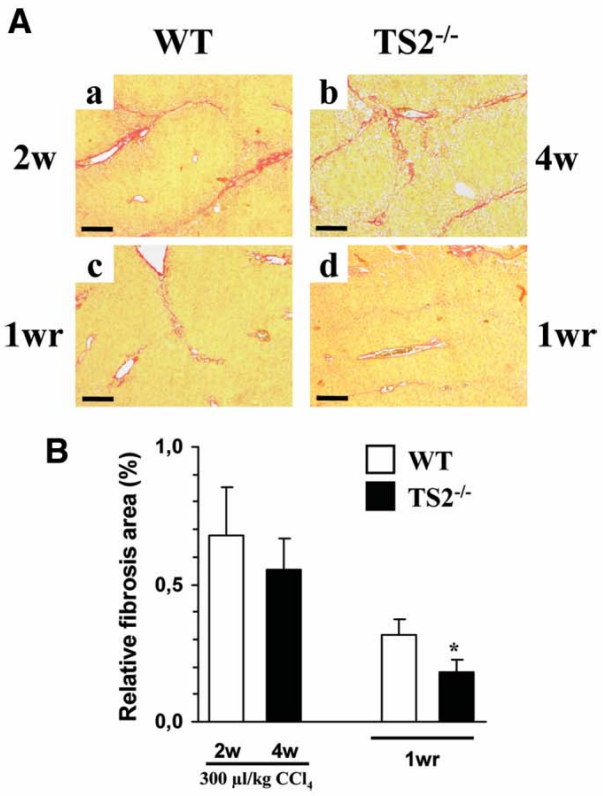

Fig. 6. Reversal of fibrosis in ADAMTS2$^{-/-}$. (A) Representative PSR staining of liver sections is shown (scale bars: 150 μm). A chronic CCl_4 treatment at a dose of 300 μL/kg in OO, as described in the Materials and Methods section, was performed (a) for 2w in WT or (b) for 4w in TS2$^{-/-}$ mice to attain a similar degree of fibrosis. (c,d) The treatment was then discontinued, and the mice were sacrificed after 1wr. (B) PSR staining was quantified by digital image analysis. The degree of fibrosis was expressed as the mean percentage ($\pm$ the SEM) of the field tissue area (n = 5-7 mice in each group). *$P < 0.05$ versus the WT mice. 1wr indicates 1 week of recovery; 2w, 2 weeks; and 4w, 4 weeks.

Regulation of the Gene Expression in WT and TS2$^{-/-}$ Mice During Fibrosis and Its Reversal. After a long-term treatment (4 weeks), most of the investigated genes were strongly up-regulated, with the exception of TGF-β1, CTGF, and α-SMA (Table 1, left) α-SMA was also assessed by immunohistology in control and fibrotic WT and TS2$^{-/-}$ livers (Fig. 7A). Besides an intense staining of the vessel walls of the portal tracts, few (but similar numbers of) α-SMA–positive cells were seen around the centrilobular veins (Fig. 7B). The mRNA levels of fibrillar collagens I, III, and V were significantly increased and similar to those recorded 4 days after a single CCl_4 injection in both genotypes. ADAMTS2 and, to a lesser extent, ADAMTS14 were increased in fibrotic WT livers. An increased expression of the investigated MMPs was noted, which was quite extensive for MMP-2, and confirmed at the protein level by zymography analyses (Supplementary Fig. 1). The up-regulation of MMP-9 was not as strong in the chronic condition as in the acute reaction. No significant difference was noted between the WT and TS2$^{-/-}$ mice. The inhibitors of MMPs, TIMP-1, TIMP-2, and TIMP-3 were also overexpressed in the fibrotic livers, but again, no significant difference was observed between WT and TS2$^{-/-}$ mice. Upon the cessation of the treatment (Table 1, right), a progressive return to a normal level of expression was observed for the fibrillar collagens and their processing and degrading enzymes. Altogether, these results show that selected gene expression in reaction to CCl_4-induced hepatic injury is similar in WT and TS2$^{-/-}$ mice.

Structural Architecture and Characterization of Newly Deposited Collagen in Fibrotic Livers. The structural architecture of newly deposited collagen in the septa was visualized with electron microscopy (Fig. 8A). In comparison with the fibrotic livers in WT mice, in

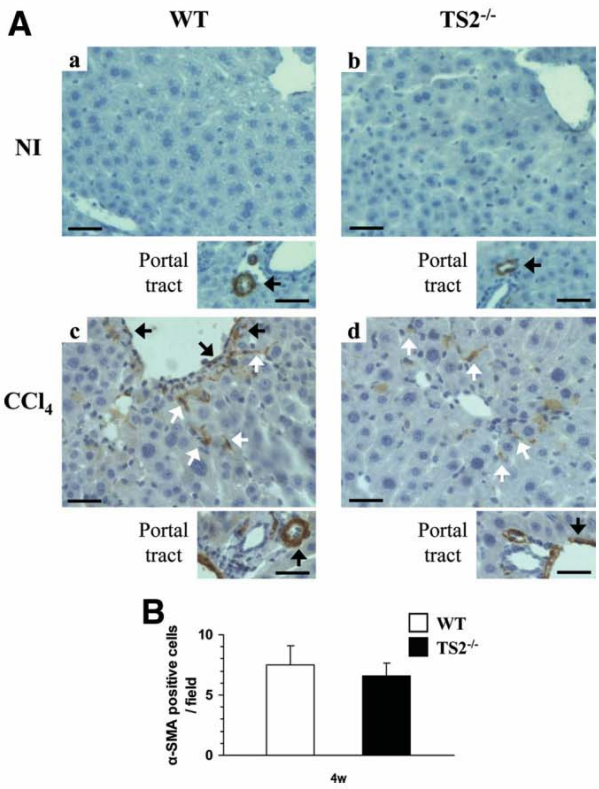

Fig. 7. Immunohistochemical staining of α-SMA. (A) Representative α-SMA immunostaining of liver sections is shown (scale bars: 50 μm). (a) NI WT mouse. (b) NI TS2$^{-/-}$ mouse. (c) WT or (d) TS2$^{-/-}$ mice subjected to a chronic 150 μL/kg CCl_4 treatment and sacrificed after 4 weeks. Besides the intense staining of the vessel walls (black arrows), α-SMA staining can be observed in elongated cells after the chronic CCl_4 treatment (white arrows). (B) The number of α-SMA-positive cells ($\pm$ SEM) was quantified in 10 fields per mouse (n = 4-5 mice in each group).

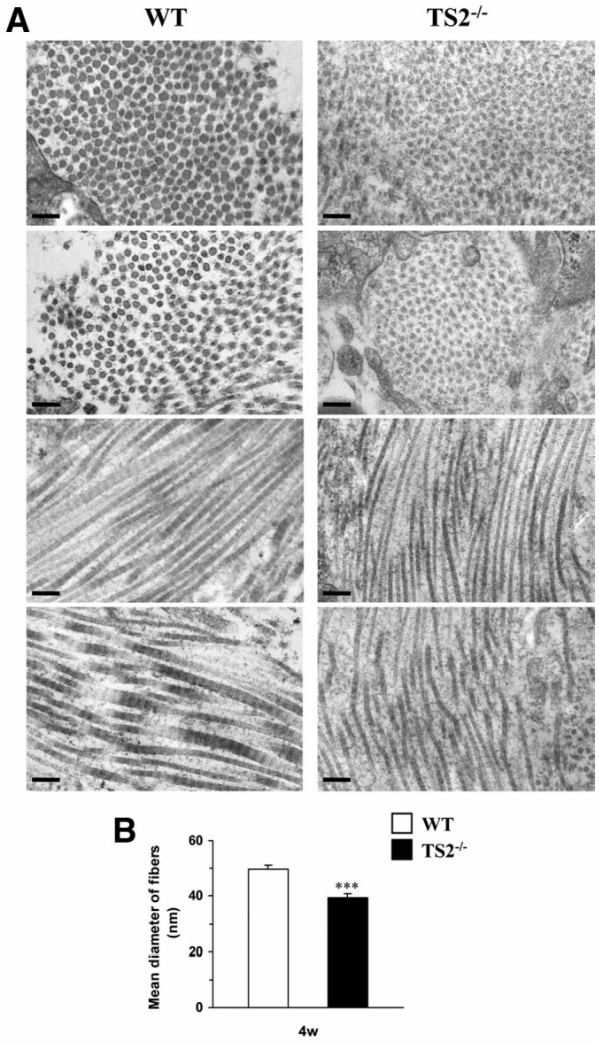

Fig. 8. Electron microscopy images of livers from WT (n = 2) and TS2$^{-/-}$ mice (n = 2) treated with CCl_4 at 300 μL/kg for 4 weeks. (A) The photographs are representative of several sections per liver in each group (scale bars: 200 nm). (B) The diameter of the fibers, measured in transverse sections in 4 fields per group, is significantly reduced in the fibrous septa of TS2$^{-/-}$ mice. ***$P < 0.001$ versus the WT mice.

which regular and cylindrical collagen fibers were parallel and were densely packed into bundles, the fibrillar collagen network in TS2$^{-/-}$ livers was less abundant and less dense. The fibers presented slightly irregular contours and a significantly smaller cross-section diameter (Fig. 8B).

The extent of processing of hepatic fibrillar pNcollagen deposited during the fibrotic process was investigated with western blotting. Figure 9A illustrates the patterns of type I collagen polypeptides extracted from the skin (lane 1) and liver (lane 3) of TS2$^{-/-}$ mice and from the same amounts of skin and liver extracts mixed together (lane 2). It first demonstrates that the anti-collagen I antibody reacted more efficiently with α2 and α2 containing the N-propeptide (pNα2) than with α1 and pNα1. Furthermore, although pNα1 was quite visible in the skin extract, it became undetectable in the mixture with the liver extract, which contained, as revealed by Coomassie blue staining (not shown), a significant amount of a liver protein displaying the same electrophoretic migration as pNα1. This protein was not affected by bacterial collagenase digestion that removed all the collagen bands nor was it affected by reduction. It was potentially identified as CPS. Its large abundance in the liver extract probably prevented the efficient transfer of pNα1 during blotting, as suggested by Fig. 9A. This protein stained by Coomassie blue was used to monitor the amount of protein loading in Fig. 9B (top panel). In nontreated animals, the α2 chain was clearly visible in WT mice and was accompanied by very little staining of α1. These protein bands were barely apparent in the TS2$^{-/-}$ mice. In CCl_4 fibrotic animals, both α1 and α2 chains were increased in the WT mice, whereas in the TS2$^{-/-}$ mice, type I collagen was lower, and only pNα2 and α2 were clearly identified. α1(III) and pNα1(III) in mouse livers were identified by a comparison with bovine purified dermatosparactic collagen III (positive control; Fig. 9C). Almost only α1(III) was observed in nontreated WT or TS2$^{-/-}$ animals. After the CCl_4 treatment, type III collagen significantly accumulated as fully processed α1(III) and little pNα1(III) in WT mice, whereas in the TS2$^{-/-}$ mice, pNα1(III) and α1(III) similarly increased.

Discussion

The excessive deposition of fibrous collagen within hepatic tissue is a frequent result of chronic injury to the liver by a number of causative agents, leading to cirrhosis as an endpoint. Effective treatments for liver fibrosis are still lacking, except for the suppression of the initial fibrogenic stimulus. The biosynthesis and polymerization of collagen, the main component of the fibrous scar, require various successive steps, thus providing a large panel of possibilities for therapeutic intervention.

In contrast to the complex regulatory events leading to fibrosis, the biosynthesis of collagen is a well-described multistep process that is quite similar in all tissues. In this study, we focused our attention on ADAMTS2, the main enzyme catalyzing the N-propeptide excision of procollagens I, III, and V,[21,32] a crucial step that allows the polymerization of the triple-helix collagen monomers to assemble and form mechanically resistant fibers and bundles. The lack of activity of ADAMTS2 is responsible for a heritable disease in humans (Ehlers-Danlos syndrome type VIIC) and animals (dermatosparaxis) characterized by extreme fragility of the skin[16,17] and other organs. Mice

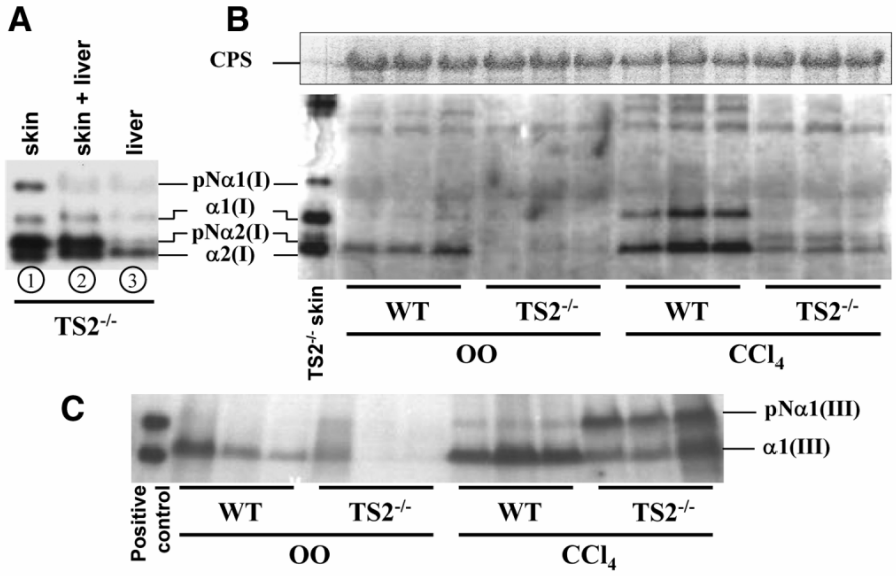

Fig. 9. Western blot analysis of type I and type III collagens. (A) Patterns of type I collagen polypeptides extracted from TS2$^{-/-}$ skin (lane 1) and liver (lane 3) with an antiserum against type I collagen are shown. In lane 2, skin and liver extracts were mixed. (B) Liver extracts of 3 WT and TS2$^{-/-}$ mice harvested after 4 weeks of an OO treatment or 300 μL/kg CCl_4 injections were submitted to western blotting with anti-type I collagen antiserum. Collagen purified from TS2$^{-/-}$ mouse skin was used as a positive control. The abundant hepatic protein (CPS) was used to monitor the amount of loaded proteins. (C) Patterns of type III collagen polypeptides in the same livers of WT and TS2$^{-/-}$ mice treated with OO or CCl_4 are shown. Purified type III collagen from dermatosparactic bovine skin containing both pNα1(III) and α1(III) chains was used as a positive control.

in which the ADAMTS2 gene has been invalidated (TS2$^{-/-}$) display the same defect in skin and some other connective tissues.[22,33] These mice were used as an *in vivo* model to evaluate a potential therapeutic benefit of inhibiting ADAMTS2 function during the development of liver fibrosis.

The acute responses of WT and TS2$^{-/-}$ mice to a single injection of CCl_4 were similar, as shown by the histology of the necrotic lesions, the serum level of hepatic enzymes, and the mRNA levels of fibrogenic cytokines, collagen, MMPs, and TIMPs. In agreement with previous reports, we observed a clear peak of overexpression of genes, such as MMP-13, MMP-9, and TIMP-1, within the first day of acute toxic liver injury in both WT and TS2$^{-/-}$ mice, which was probably related to the release of inflammatory cytokines.[34] A similar peak of TIMP-3 was observed 1 day after injury in the WT mice. It could be regarded as an acute phase protein together with TIMP-1.[35] Besides its activity as an inhibitor of MMPs, TIMP-3 controls the activity of ADAM metallopeptidase domain 17, a pro–tumor necrosis factor α processing enzyme. Its lack of activity in TIMP-3 null mice leads to chronic hepatic inflammation and failure of liver regeneration.[36] Its higher induction in WT may be related to ADAMTS2 activity on novel substrates that are under investigation.

PSR staining evaluated by automated digital image analysis, hydroxyproline content quantification, and a transcriptomic analysis of a large series of genes potentially participating in the remodeling process were used to assess the development of fibrosis upon chronic exposure to CCl_4 and its resolution. All investigated parameters of the liver response to chronic injury were also similarly modulated in WT and TS2$^{-/-}$ animals. It was clearly demonstrated that TS2$^{-/-}$ mice developed less extensive hepatic fibrosis than their WT littermates, and this was related to a slower rate of deposition of poorly structured fibrils of partly processed collagen precursors.

The edification of a fibrous collagen matrix is a complex process of remodeling regulated by a positive balance between the production of new structures and their degradation. This balance is clearly illustrated by the steady-state level of the mRNA; both the WT and the TS2$^{-/-}$ animals display a large and similar increase in collagen mRNAs. The degrading enzymes are also quite similarly increased. The removal of such structures during, for example, fibrosis resolution operates by similar mechanisms in which degradation is greater than deposition. The increased expression of the genes for producing matrix collagens I and III and that of the genes involved in their degradation are similarly modulated in WT and TS2$^{-/-}$ mice. Collectively, these results indicate that the reduced fibrosis in TS2$^{-/-}$ mice is not due to reduced collagen synthesis or up-regulation of proteolytic enzymes but

seems directly related to the absence of ADAMTS2 activity responsible for the persistence of the N-propeptide in a significant proportion of type I and III collagen molecules. The steric hindrance introduced by the N-propeptide leads to delayed and/or altered assembly of collagen molecules into fibrils and the formation of thinner and loosely packed fibers. The structural alterations are, however, less marked than those observed in the skin of human beings suffering from Ehlers-Danlos syndrome type VIIC, dermatosparactic animals, and $TS2^{-/-}$ mice.[16,22] These poorly organized polymers are more susceptible to degradation by collagenase (F.K., unpublished data, 2007). This hypothesis is largely supported by the observation that transgenic mice expressing a mutated collagen resistant to collagenase degradation display a higher level of hepatic fibrosis.[37]

An alternative model for inducing a fibrotic reaction in the liver by ligation of the bile duct[23,38] was also investigated. The extreme fragility of the connective tissues in $TS2^{-/-}$ mice caused early tears in the distended bile duct walls and a high mortality rate before the long-term development of fibrosis. However, a few animals could be sacrificed 9 days after BDL. In WT mice, extensive bile duct proliferation around portal tracts was accompanied by fibrous PSR-stained extensions within the hepatic parenchyma. In $TS2^{-/-}$ mice, however, the PSR staining around the bile ducts in the portal tract was lighter than that in the WT mice, and no fibrotic extension was observed toward the hepatic tissue. This observation is consistent with the reduced fibrosis observed in $TS2^{-/-}$ mice in the CCl_4 model.

ADAMTS2, ADAMTS3, and ADAMTS14 are the 3 proteases responsible for the pNcollagen peptidase activity in the organism.[12] ADAMTS3 expression was not detected in the livers of our mice, whereas ADAMTS14, expressed and stimulated by CCl_4, may compensate for the absence of ADAMTS2, explaining partial processing of the pNcollagen in the $TS2^{-/-}$ livers. The simultaneous inhibition of the 2 pNcollagen peptidases by the use of small interfering RNA or blocking antibodies directed against their catalytic site, for example, would probably prevent processing of the N-propeptide of all fibrillar collagens, resulting in an even higher instability of the collagen fibers. Targeted activation of TIMP-3, recently identified as an inhibitor of ADAMTS2 *in vitro*,[39] may represent an alternative approach.

The inhibition of fibrosis by targeting the far end of its development through the reduction of the stability of fibrous collagen, as described in this article, seems to be a safe strategy. Indeed, the physiological turnover of collagen in adults is a very slow process in comparison with collagen remodeling during fibrogenesis. The side effects resulting from the inhibition of ADAMTS2 activity should therefore be limited and probably fully reversible at the end of the treatment. Reducing collagen stability has already been investigated with inhibitors of prolyl-4-hydroxylase, the enzyme catalyzing the formation of hydroxyprolyl residues responsible for the collagen triple-helix stabilization. The tested inhibitors of prolyl-4-hydroxylase effectively inhibited experimental fibrosis development,[40,41] and this supported the concept of post-translational modifications of procollagen as suitable targets for therapeutic intervention.

In conclusion, the suppression of ADAMTS2, a critical metalloproteinase for collagen maturation and stabilization, reduces hepatic fibrosis *in vivo*. Strategies to knock down its expression or activity in the liver may be considered alternative, effective, and basically only slightly aggressive antifibrotic therapies.

Acknowledgment: We gratefully thank J. Delwaide for his interest and advice and M.-J. Nix and T. Heyeres for their expert technical assistance.

References

1. Schuppan D. Structure of the extracellular matrix in normal and fibrotic liver: collagens and glycoproteins. Semin Liver Dis 1990;10:1-10.
2. Desmet VJ, Roskams T. Cirrhosis reversal: a duel between dogma and myth. J Hepatol 2004;40:860-867.
3. Olaso E, Friedman SL. Molecular regulation of hepatic fibrogenesis. J Hepatol 1998;29:836-847.
4. Bissel DM, Maher JJ. Hepatic fibrosis and cirrhosis. In: Zakim D, Boyer TD, eds. Hepatology: A Textbook of Liver Disease. Philadelphia, PA: Saunders, 1996:506-525.
5. Bataller R, Brenner DA. Liver fibrosis. J Clin Invest 2005;115:209-218.
6. Tsukada S, Parsons CJ, Rippe RA. Mechanisms of liver fibrosis. Clin Chim Acta 2006;364:33-60.
7. Li SW, Sieron AL, Fertala A, Hojima Y, Arnold WV, Prockop DJ. The C-proteinase that processes procollagens to fibrillar collagens is identical to the protein previously identified as bone morphogenic protein-1. Proc Natl Acad Sci U S A 1996;93:5127-5130.
8. Kessler E, Takahara K, Biniaminov L, Brusel M, Greenspan DS. Bone morphogenetic protein-1: the type I procollagen C-proteinase. Science 1996;271:360-362.
9. Lapiere CM, Lenaers A, Kohn LD. Procollagen peptidase: an enzyme excising the coordination peptides of procollagen. Proc Natl Acad Sci U S A 1971;68:3054-3058.
10. Colige A, Li SW, Sieron AL, Nusgens BV, Prockop DJ, Lapiere CM. cDNA cloning and expression of bovine procollagen I N-proteinase: a new member of the superfamily of zinc-metalloproteinases with binding sites for cells and other matrix components. Proc Natl Acad Sci U S A 1997; 94:2374-2379.
11. Fernandes RJ, Hirohata S, Engle JM, Colige A, Cohn DH, Eyre DR, et al. Procollagen II amino propeptide processing by ADAMTS-3. Insights on dermatosparaxis. J Biol Chem 2001;276:31502-31509.
12. Colige A, Vandenberghe I, Thiry M, Lambert CA, Van Beeumen J, Li SW, et al. Cloning and characterization of ADAMTS-14, a novel ADAMTS displaying high homology with ADAMTS-2 and ADAMTS-3. J Biol Chem 2002;277:5756-5766.
13. Lapiere CM, Nusgens B. Polymerization of procollagen in vitro. Biochim Biophys Acta 1974;342:237-246.

14. Hulmes DJ, Kadler KE, Mould AP, Hojima Y, Holmes DF, Cummings C, et al. Pleomorphism in type I collagen fibrils produced by persistence of the procollagen N-propeptide. J Mol Biol 1989;210:337-345.
15. Pierard GE, Le T, Hermanns JF, Nusgens BV, Lapiere CM. Morphometric study of cauliflower collagen fibrils in dermatosparaxis of the calves. Coll Relat Res 1987;6:481-492.
16. Nusgens BV, Verellen-Dumoulin C, Hermanns-Le T, De Paepe A, Nuytinck L, Pierard GE, et al. Evidence for a relationship between Ehlers-Danlos type VII C in humans and bovine dermatosparaxis. Nat Genet 1992;1:214-217.
17. Colige A, Sieron AL, Li SW, Schwarze U, Petty E, Wertelecki W, et al. Human Ehlers-Danlos syndrome type VII C and bovine dermatosparaxis are caused by mutations in the procollagen I N-proteinase gene. Am J Hum Genet 1999;65:308-317.
18. Colige A, Nuytinck L, Hausser I, van Essen AJ, Thiry M, Herens C, et al. Novel types of mutation responsible for the dermatosparactic type of Ehlers-Danlos syndrome (type VIIC) and common polymorphisms in the ADAMTS2 gene. J Invest Dermatol 2004;123:656-663.
19. Tuderman L, Kivirikko KI, Prockop DJ. Partial purification and characterization of a neutral protease which cleaves the N-terminal propeptides from procollagen. Biochemistry (Mosc) 1978;17:2948-2954.
20. Wang WM, Lee S, Steiglitz BM, Scott IC, Lebares CC, Allen ML, et al. Transforming growth factor-beta induces secretion of activated ADAMTS-2. A procollagen III N-proteinase. J Biol Chem 2003;278:19549-19557.
21. Colige A, Ruggiero F, Vandenberghe I, Dubail J, Kesteloot F, Van Beeumen J, et al. Domains and maturation processes that regulate the activity of ADAMTS-2, a metalloproteinase cleaving the aminopropeptide of fibrillar procollagens types I-III and V. J Biol Chem 2005;280:34397-34408.
22. Li SW, Arita M, Fertala A, Bao Y, Kopen GC, Langsjo TK, et al. Transgenic mice with inactive alleles for procollagen N-proteinase (ADAMTS-2) develop fragile skin and male sterility. Biochem J 2001;355:271-278.
23. Ezure T, Sakamoto T, Tsuji H, Lunz JG III, Murase N, Fung JJ, et al. The development and compensation of biliary cirrhosis in interleukin-6-deficient mice. Am J Pathol 2000;156:1627-1639.
24. Bergman I, Loxley R. Two improved and simplified methods for the spectrophotometric determination of hydroxyproline. Anal Chem 1963;35:1961-1965.
25. Waldrop FS, Puchtler H. Light microscopic distinction of collagens in hepatic cirrhosis. Histochemistry 1982;74:487-491.
26. Laemmli UK. Cleavage of structural proteins during the assembly of the head of bacteriophage T4. Nature 1970;227:680-685.
27. Towbin H, Staehelin T, Gordon J. Electrophoretic transfer of proteins from polyacrylamide gels to nitrocellulose sheets: procedure and some applications. Proc Natl Acad Sci U S A 1979;76:4350-4354.
28. Paye M, Etievant C, Michiels F, Pierard D, Nusgens B, Lapiere CM. Characterization of a spontaneously transformed pulmonary embryonic rat (PER) epithelial cell line. J Cell Sci 1986;86:83-93.
29. Lambert CA, Colige AC, Lapiere CM, Nusgens BV. Coordinated regulation of procollagens I and III and their post-translational enzymes by dissipation of mechanical tension in human dermal fibroblasts. Eur J Cell Biol 2001;80:479-485.
30. Lambert CA, Colige AC, Munaut C, Lapiere CM, Nusgens BV. Distinct pathways in the over-expression of matrix metalloproteinases in human fibroblasts by relaxation of mechanical tension. Matrix Biol 2001;20:397-408.
31. Nakamura K, Nonaka H, Saito H, Tanaka M, Miyajima A. Hepatocyte proliferation and tissue remodeling is impaired after liver injury in oncostatin M receptor knockout mice. HEPATOLOGY 2004;39:635-644.
32. Colige A, Beschin A, Samyn B, Goebels Y, Van Beeumen J, Nusgens BV, et al. Characterization and partial amino acid sequencing of a 107-kDa procollagen I N-proteinase purified by affinity chromatography on immobilized type XIV collagen. J Biol Chem 1995;270:16724-16730.
33. Le Goff C, Somerville RP, Kesteloot F, Powell K, Birk DE, Colige AC, et al. Regulation of procollagen amino-propeptide processing during mouse embryogenesis by specialization of homologous ADAMTS proteases: insights on collagen biosynthesis and dermatosparaxis. Development 2006;133:1587-1596.
34. Hemmann S, Graf J, Roderfeld M, Roeb E. Expression of MMPs and TIMPs in liver fibrosis—a systematic review with special emphasis on anti-fibrotic strategies. J Hepatol 2007;46:955-975.
35. Yata Y, Takahara T, Furui K, Zhang LP, Watanabe A. Expression of matrix metalloproteinase-13 and tissue inhibitor of metalloproteinase-1 in acute liver injury. J Hepatol 1999;30:419-424.
36. Mohammed FF, Smookler DS, Taylor SE, Fingleton B, Kassiri Z, Sanchez OH, et al. Abnormal TNF activity in Timp3−/− mice leads to chronic hepatic inflammation and failure of liver regeneration. Nat Genet 2004;36:969-977.
37. Issa R, Zhou X, Trim N, Millward-Sadler H, Krane S, Benyon C, et al. Mutation in collagen-1 that confers resistance to the action of collagenase results in failure of recovery from CCl4-induced liver fibrosis, persistence of activated hepatic stellate cells, and diminished hepatocyte regeneration. FASEB J 2003;17:47-49.
38. Xia JL, Dai C, Michalopoulos GK, Liu Y. Hepatocyte growth factor attenuates liver fibrosis induced by bile duct ligation. Am J Pathol 2006;168:1500-1512.
39. Wang WM, Ge G, Lim NH, Nagase H, Greenspan DS. TIMP-3 inhibits the procollagen N-proteinase ADAMTS-2. Biochem J 2006;398:515-519.
40. Bickel M, Baringhaus KH, Gerl M, Gunzler V, Kanta J, Schmidts L, et al. Selective inhibition of hepatic collagen accumulation in experimental liver fibrosis in rats by a new prolyl 4-hydroxylase inhibitor. HEPATOLOGY 1998;28:404-411.
41. Sakaida I, Uchida K, Hironaka K, Okita K. Prolyl 4-hydroxylase inhibitor (HOE 077) prevents TIMP-1 gene expression in rat liver fibrosis. J Gastroenterol 1999;34:376-377.

Supplementary table 1. Primer sequences and number of cycles used for quantification of mouse hepatic mRNA levels by RT-PCR.

Gene	Sequence of primers		No of cycles
Coll α1(I)	Forward	5'-CCCTGAAGTCAGCTGCATACACAA-3'	32
	Reverse	5'-CCTACATCTTCTGAGTTTGGTGAT-3'	
Coll α1(III)	Forward	5'-GAGATGTCTGGAAGCCAGAACCAT-3'	30
	Reverse	5'-GATCTCCCTTGGGGCCTTGAGGT-3'	
Coll α1(V)	Forward	5'-GGAAGAGATCTTTGGTTCCCTCAA-3'	30
	Reverse	5'-AAGTGATTCTGGCTCCCTCAGACT-3'	
TGF-β1	Forward	5'-CGGTGCTCGCTTTGTACAACAGCA-3'	32
	Reverse	5'-CTGCTTCCCGAATGTCTGACGTA-3'	
CTGF	Forward	5'-TCTCCACCCGAGTTACCAATGACA-3'	32
	Reverse	5'-ACCCCGCAGAACTTAGCCCTGTA-3'	
α-SMA	Forward	5'-CGACACTGCTGACAGAGGCACCA-3'	31
	Reverse	5'-ATAGGCACGTTGTGAGTCACACCA-3'	
MMP-2	Forward	5'-AGATCTTCTTCTTCAAGGACCGGTT-3'	27
	Reverse	5'-GGCTGGTCAGTGGCTTGGGGTA-3'	
MMP-9	Forward	5'-GTTTTTGATGCTATTGCTGAGATCCA-3'	35
	Reverse	5'-CCCACATTTGACGTCCAGAGAAGAA-3'	
MMP-13	Forward	5'-ATGATCTTTAAAGACAGATTCTTCTGG-3'	35
	Reverse	5'-TGGGATAACCTTCCAGAATGTCATAA-3'	
MMP-14	Forward	5'-GGATACCCAATGCCCATTGGCCA-3'	25
	Reverse	5'-CCATTGGGCATCCAGAAGAGAGC-3'	
TIMP-1	Forward	5'-GGCATCCTCTTGTTGCTATCACTG-3'	27
	Reverse	5'-GTCATCTTGATCTCATAACGCTGG-3'	
TIMP-2	Forward	5'-CTCGCTGGACGTTGGAGGAAAGAA-3'	27
	Reverse	5'-AGCCCATCTGGTACCTGTGGTTCA-3'	
TIMP-3	Forward	5'-CTTCTGCAACTCCGACATCGTGAT-3'	29
	Reverse	5'-CAGCAGGTACTGGTACTTGTTGAC-3'	
ADAMTS2	Forward	5'-CAGCCGCTACCTGCATTCCTATGA-3'	32
	Reverse	5'-CAGGCGCACACATAGTACCATCCA-3'	
ADAMTS14	Forward	5'-AGCCTGGCCTACAAGTACGTCAT-3'	35
	Reverse	5'-CTCCTCCACAGGCCTTGCTGCA-3'	
28S rRNA	Forward	5'-GTTCACCCACTAATAGGGAACGTGA-3'	17
	Reverse	5'-GATTCTGACTTAGAGGCGTTCAGT-3'	

α1(III), α1 chain of type III collagen; TGF-β1; transforming growth factor-beta 1; CTGF, connective tissue growth factor; α-SMA, alpha-smooth muscle actin; MMP, matrix metalloproteinase; TIMP, tissue inhibitor of metalloproteinases; ADAMTS, A Disintegrin And Metalloprotease domain with ThromboSpondin type I repeats.

1

Supplementary figure 1. Gelatin zymography of liver homogenates. (A) Gelatinolytic activity of proMMP-2 and proMMP-9 in the liver of WT and TS2$^{-/-}$ mice harvested after 4 weeks of OO treatment and 150 µl/kg or 300 µl/kg CCl_4 injections. Serum-free medium conditioned by human fibrosarcoma HT1080 cells was used as a positive control. (B) Quantification by digital image analysis. Results are expressed as the mean (+ SEM) of groups of 4 mice. A significant increase was observed upon CCl_4 treatment at both concentrations in WT and TS2$^{-/-}$ mice. At 300 µl/kg, a slight increase of proMMP-2 is observed in TS2$^{-/-}$ mice (*, $P < 0.05$). No activated proMMP-9 or proMMP-2 was detected in the livers.